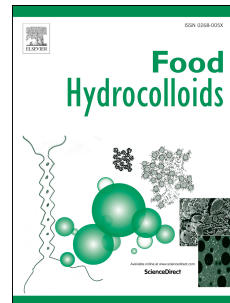


Accepted Manuscript

Links between particle surface hardening and rehydration impairment during micellar casein powder storage

Jennifer Burgain, Joël Scher, Jeremy Petit, Gregory Francius, Claire Gaiani



PII: S0268-005X(16)30218-1

DOI: [10.1016/j.foodhyd.2016.05.021](https://doi.org/10.1016/j.foodhyd.2016.05.021)

Reference: FOOHYD 3434

To appear in: *Food Hydrocolloids*

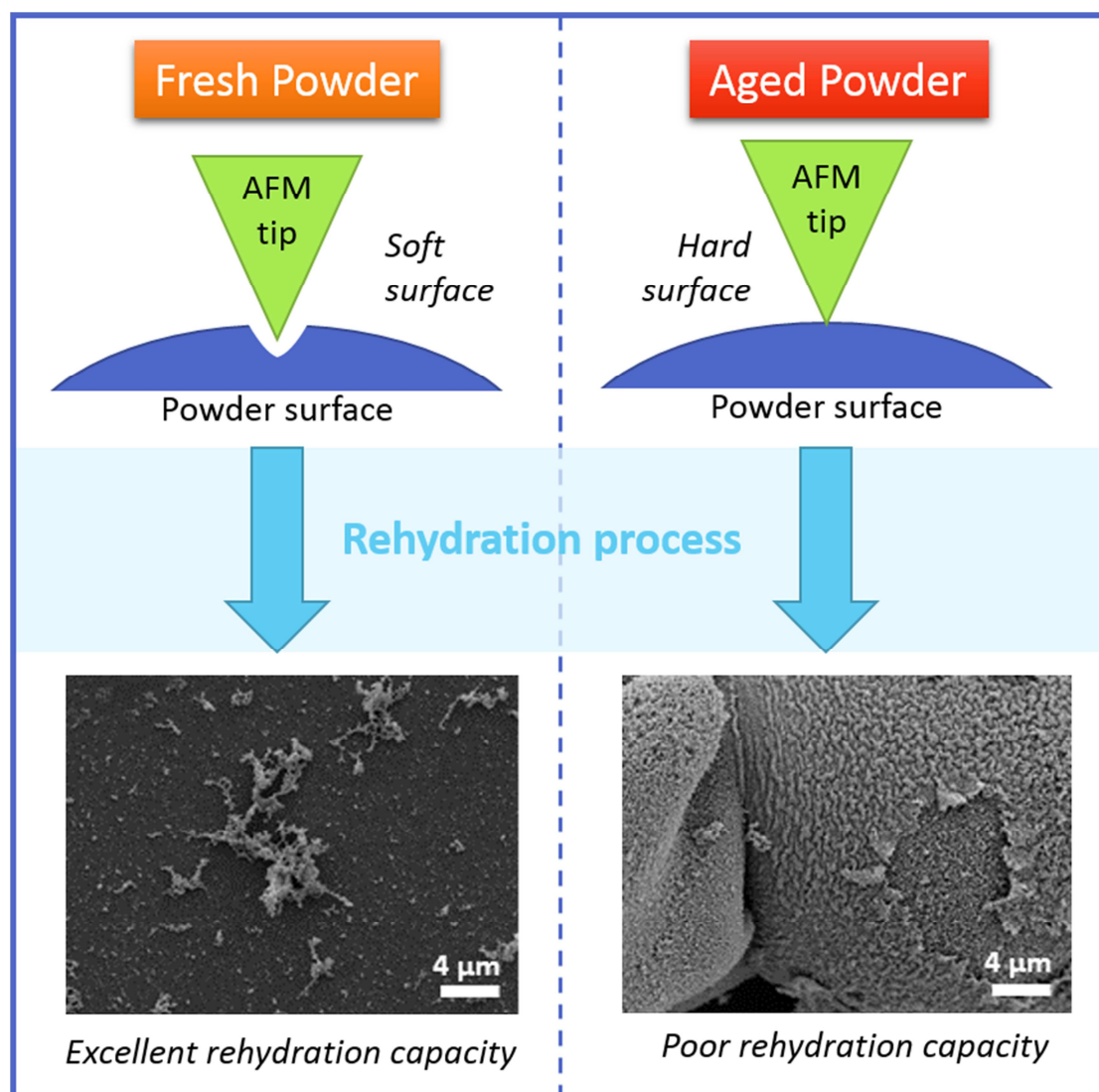
Received Date: 16 March 2016

Revised Date: 11 May 2016

Accepted Date: 19 May 2016

Please cite this article as: Burgain, J., Scher, J., Petit, J., Francius, G., Gaiani, C., Links between particle surface hardening and rehydration impairment during micellar casein powder storage, *Food Hydrocolloids* (2016), doi: 10.1016/j.foodhyd.2016.05.021.

This is a PDF file of an unedited manuscript that has been accepted for publication. As a service to our customers we are providing this early version of the manuscript. The manuscript will undergo copyediting, typesetting, and review of the resulting proof before it is published in its final form. Please note that during the production process errors may be discovered which could affect the content, and all legal disclaimers that apply to the journal pertain.



1 Links between particle surface hardening and rehydration impairment during micellar casein
2 powder storage

3

4 BURGAIN Jennifer^{a,b*}, SCHER Joël^b, PETIT Jeremy^b, FRANCIUS Gregory^c, and GAIANI
5 Claire^{b,d*}

6

7 ^a CNIEL, 42 rue de Châteaudun, 75314 Paris Cedex 9, France.

8 ^b Université de Lorraine, LIBio, Laboratoire d'Ingénierie des Biomolécules, 2 avenue de la
9 Forêt de Haye, TSA 40602, 54518 Vandœuvre-lès-Nancy cedex, France.

10 ^c Université de Lorraine, LCPME, Laboratoire de Chimie Physique et Microbiologie pour
11 l'Environnement, UMR 7564, 54600 Villers-lès-Nancy, France.

12 ^d The University of Queensland, School of Agricultural and Food Science, St. Lucia, Qld.
13 4072, Australia.

14

15

16 * Corresponding author. Tel.: +33-3-83-59-58-78; Fax: +33-3-83-59-58-04.

17 E-mail address: claire.gaiani@univ-lorraine.fr (C. Gaiani)

18

19

20 **Abstract**

21 Storage is an unavoidable critical phase regarding dairy powder reconstitution abilities,
22 particularly for high casein content powders, which generally present a poor rehydration
23 behavior. The ability of micellar casein powders to completely rehydrate can thus be
24 particularly affected by storage time and temperature. To implement best practices for the
25 optimization of storage conditions, understanding changes occurring is a crucial point. For the
26 first time, biophysical techniques were used to investigate powder surface at the nanoscale.
27 Atomic force microscopy revealed that particle surface became rougher during storage,
28 associated with the formation of hollow zones (around 500 nm) holes when stored for 10
29 months at 40 °C. Mechanical properties of micellar casein particle surface during powder
30 storage was quantified using AFM nanoindentation. Spatially-resolved force/indentation
31 curves evidenced a significant stiffer surface for aged powder (Young modulus of ~20 GPa)
32 in comparison with the fresh one (~0.2 GPa). These findings were fully consistent with the
33 formation of a crust at the powder surface observed by high-resolution field-emission
34 scanning electron microscopy during powder rehydration. Finally, alterations of the
35 rehydration process can be related to modifications occurring at the particle surface during
36 storage.

37

38

39 **Keywords:** AFM; nanoindentation; surface characterization; micellar casein powder, SEM

40

41

42 1. Introduction

43 High-protein dairy powders are ingredients added to a large variety of products in
44 order to improve food nutritional, functional and/or sensory properties (Kelly & Fox, 2016).
45 The ability of dehydrated dairy ingredients to rehydrate readily in aqueous media is essential
46 if their underlying functionality is to be exploited (Crowley, Kelly, Schuck, Jeantet &
47 O'mahony, 2016; Fang, Selomulya, Ainsworth, Palmer & Chen, 2011; Gaiani, Schuck, Scher,
48 Desobry & Banon, 2007; Mimouni, Deeth, Whittaker, Gidley & Bhandari, 2009; Mimouni,
49 Deeth, Whittaker, Gidley & Bhandari, 2010b). Concerning high-protein powders concentrated
50 in caseins, poor rehydration characteristics in aqueous media are often encountered. In
51 addition, intrinsic powder properties, such as surface and bulk composition, particle structure
52 (*e.g.* morphology, presence of pores and capillaries) and rehydration conditions (*e.g.* stirring
53 rate, temperature, solids content), can influence rehydration behavior (Crowley et al., 2016).
54 Micellar casein (MC) powders belongs to high protein dairy powders, they are produced by
55 membrane filtration of skimmed milk followed by spray-drying (Schuck et al., 1994; Rollema
56 & Muir, 2009). In these powders, whey proteins are removed and caseins are present under a
57 micellar state (casein micelles containing colloidal calcium phosphate). Formation of inter-
58 linked network of casein micelles at the particle surfaces during processing can explain the
59 poor rehydration capacity of such powders. Dispersion of the powder into primary particles is
60 the limiting step to allow complete rehydration after a reasonable period of time (Anema et
61 al., 2006; Havea, 2006; Baldwin, 2010; Fang et al., 2012; Haque et al., 2012; Crowley et al.,
62 2016). Moreover, the rehydration capacity decrease is linked to storage conditions
63 (temperature, water activity, duration, etc.) and fresh powders present better rehydration
64 properties than aged powders (Fang et al., 2011; Gazi & Huppertz 2015). For example, higher
65 storage temperature leads to a decrease in MPC (milk protein concentrate) powders solubility
66 (Anema, Pinder, Hunter & Hemar, 2006; Fang et al., 2011; Fyfe et al., 2011; Gazi & Huppertz

67 2015) and the caseins dominate the composition of insoluble material (Anema et al., 2006).
68 Also, the quantity of insoluble material was increased at high relative humidity (Le, Bhandari
69 & Deeth, 2011) and linked to the apparition of Maillard products (Le, Bhandari, Holland &
70 Deeth, 2011). However, covalent cross-linking explanation as the cause of insolubility
71 development is questionable (Gazi and Huppertz, 2015) because prolonged reconstitution
72 times eventually lead to full solubility of MPC powders (Mimouni et al., 2010a). Finally, the
73 composition of particle surface plays a crucial role in powder rehydration as it was supported
74 by XPS analysis (increase in non-polar bonding) (Gaiani et al., 2006) and by Atomic Force
75 Microscopy (AFM) where MPC established attractive forces with a hydrophobic surface
76 (Fyfe et al., 2011). Decrease in rehydration was also attributed to compounds migration from
77 particle core to surface during storage. MC powder is mainly composed of caseins and only
78 residual phospholipids were found to migrate to the surface (Gaiani et al., 2006; Gaiani et al.,
79 2007).

80

81 Dairy powder surface in depth investigation appears essential to elucidate the nature of
82 phenomena occurring. In the pharmaceutical field, development of new techniques able to
83 probe surface mechanical properties of the powders were recently implemented (Wu, Li &
84 Mansour, 2010). Among these techniques, AFM nanoindentation allows measurements on
85 individual particles while providing mechanical properties at nanometer scale. Indentation
86 testing is a method consisting in touching the surface of interest presenting unknown
87 mechanical properties such as elastic modulus and hardness with another material presenting
88 knowns properties. Mechanical properties of milk protein skin layers after drying were
89 estimated by indentation test in order to understand the mechanisms of particle formation but
90 was not directly performed on particle powder and at a nanoscale (Sadek et al., 2015).
91 Nanoindentation is an indentation test in which the length scale of the penetration is measured

92 in nanometers rather than microns or millimeters, the latter being common in conventional
93 hardness tests (Fischer-Cripps, 2000). Nanoindentation can be performed with an atomic force
94 microscope and the interesting advantages of the technique are to get a mapping of elastic
95 modulus on a defined region. This particular case give local information of surface hardness.
96 A cantilever force sensor is very reliable and sensitive which makes the AFM an ideal tool for
97 probing by this sensor, the mechanical properties of materials with high resolution and high
98 sensitivity. Such characterizations can be obtained by performing a force-distance curve. By
99 analyzing the force curve approach with theoretical models, the mechanical properties (*ie*
100 stiffness, Young's modulus) of the soft sample can be obtained (Kasas, Longo and Dietler,
101 2013). In the field of pharmaceutical materials, nanoindentation was for example performed
102 on lactose (Masterson & Cao, 2008; Perkins et al., 2007) or sucrose (Liao & Wiedmann,
103 2004; Masterson et al., 2008; Ramos & Bahr, 2007). Pharmaceutical powders were
104 characterized by AFM nanoindentation in order to correlate particle hardness with powder
105 compaction performance (Cao, Morganti, Hancock & Masterson, 2010). On the best
106 knowledge of the authors, a declination of these promising biophysical techniques to food
107 powders was never done. Given that crust formation has been reported during process and
108 storage, nanomechanical measurements appear as an interesting tool to evaluate very local
109 modifications of particle powder surface. Even if the method was used from several decades
110 for pharmaceutical application, it was never applied for dairy powders. In this context, the
111 present study aimed at understanding how particle surface is modified at nanoscale during
112 storage at high temperature and the consequence of these structural alterations on the
113 hydration mechanism of particle surface during powder rehydration.

114

115 **2. Material and methods**

116 **2.1. MC powders: production and storage**

117 MC concentrate was provided by a dairy company (Ingredia, France). It was obtained
118 from skimmed milk by tangential membrane microfiltration followed by purification through
119 water diafiltration (Pierre, Fauquant, Le Graet, Piot & Maubois, 1992; Schuck et al., 1994).
120 The concentrate was spray-dried at Bionov (Rennes, France) in a three-stage pilot-plant spray-
121 dryer (GEA, Niro Atomizer, St Quentin en Yvelines, France). The inlet and outlet
122 temperatures were fixed at 150 °C and 50 °C respectively. MC powders were packaged in
123 sealed tins ($a_w = 0.2$), then stored under a controlled temperature of 40 °C for ten months.
124 This high temperature was chosen to enhance physicochemical phenomena observed during
125 powder storage.

126

127 **2.2. Rehydration protocol**

128 Rehydration was performed at 5 % (w/v) powder concentration in water. 0.5 g MC
129 powder was added to 10 mL deionised water. Stirring (200 rpm) at ambient temperature was
130 carried out for 5 min (short-term rehydration) and 60 min (long-term rehydration).

131

132 **2.3. Surface observation**

133 **2.3.1. Scanning Electron Microscopy**

134 A high-resolution field-emission scanning electron microscopy (SEM) type JEOL
135 JSM-7100F supplied with a hot (Schottky) electron gun (JEOL Ltd., Tokyo, Japan) and
136 having a resolution around 1 nm at 30 kV was used to investigate the surface morphology and
137 structure of MC powders. Powder particle surface observation during rehydration was
138 conducted according to the protocol developed by Mimouni et al. (Mimouni, Deeth,
139 Whittaker, Gidley & Bhandari, 2010a) with small modifications. The suspension containing
140 powder particles (under short or long-term rehydration) was deposited on a silicon chip wafer
141 (ProSciTech, Kirwan, Australia) that has previously been coated with poly-L-Lys (Sigma,

142 Castle Hill, Australia). Powder particles were able to adhere to the wafer by creating
143 electrostatic bonds with the substrate. The suspension was kept in contact with the wafer for 5
144 min, then the wafer was drained and rinsed with 100 mM phosphate buffer (pH = 7).
145 Chemical protein fixation was achieved by immersing the wafer in a solution composed of 3
146 % glutaraldehyde in 100 mM phosphate buffer (pH = 7) for 15 min. When the fixation was
147 completed, the samples were gently washed in phosphate buffer and dehydrated using the
148 following graded ethanol series: 50 %, 60 %, 70 %, 80 %, 90 % (1 time) and 100% (3 times).
149 The elapsed time per solution was 3 min (Dalglish, Spagnuolo & Goff, 2004). Samples were
150 then dried by using CO₂ in a Supercritical Autosamdri-815B critical point dryer (Tousimis,
151 Rockville, MD, USA). The silicon wafer was then mounted onto electron microscopy stubs
152 thanks to a carbon double-sided adhesive tape. Finally, samples were coated with iridium
153 (Q150T Turbo-Pumped Sputter Coater, ProSciTech Pty Ltd, Australia) for 2 min (~ 15 nm
154 thick).

155

156 **2.3.2. AFM: surface topography and roughness**

157 Dairy powders were fixed onto a circular glass thanks to epoxy glue. AFM measurements
158 were performed at room temperature using an Asylum MFP-3D atomic force microscope
159 (Santa Barbara, CA, USA) with IGOR Pro 6.04 operation software (Wavemetrics, Lake
160 Osewego, OR, USA). All images were acquired in liquid media, more precisely in ethanol to
161 avoid powder rehydration during experiments. Topography images were obtained in contact
162 mode at 1 Hz scan rate with NPG-10 gold cantilevers (Bruker AXS, Palaiseau, France). The
163 scanned surface area was of 5 $\mu\text{m} \times 5 \mu\text{m}$ corresponding to 512 points \times 512 lines. The
164 average roughness (R_a) was calculated for MC powder particles with the following
165 expression:

$$R_a = \frac{1}{L_x L_y} \int_0^{L_y} \int_0^{L_x} |f(x, y)| dx dy \quad (1)$$

166 Where $f(x, y)$ is the surface relative to the center plane, L_x and L_y are the dimensions of the
167 surface. Tukey test was performed using KyPlot software version 2.0 in order to determine
168 significant differences. To this end, roughness of around ten images was used to perform
169 statistical analyses.

170

171 **2.4. Surface characterization**

172 **2.4.1. XPS**

173 Elemental composition of the surface layer of MC powder (up to 5 - 6 nm depth) was
174 measured by X-ray Photoelectron Spectroscopy (XPS) (Gaiani et al., 2006; Rouxhet et al.,
175 2008). Prior to analysis, the sample was outgassed under vacuum for 24 h. Spectra were
176 obtained with a KRATOS Axis Ultra X-ray photoelectron spectrometer (Kratos Analytical,
177 Manchester, UK) equipped with a monochromatic Al $K\alpha$ X-ray ($h\nu = 1486.6$ eV) operated at
178 150 W. Spectra were collected at normal take-off angle (90°) and the analysis area was 700
179 $\mu\text{m} \times 300 \mu\text{m}$.

180

181 **2.4.2 AFM Nanoindentation**

182 Mechanical properties of dairy powder particle surface were obtained in three steps
183 described in **Figure 1**.

184 (1) First of all, particle powders were spread onto a thin coat of epoxy glue deposited on
185 the surface of a cleaned circular glass and the overall was let overnight to allow glue
186 hardening.

187 AFM measurements were performed with a diamond tip of Berkovich type purchased from
188 Veeco (DNISP, Veeco Instruments SAS, Palaiseau, France). Regarding the cantilever, the

189 DNISP spring constant k_c was evaluated at about 300 N.m^{-1} by the thermal calibration method
190 (Levy & Maaloum, 2002). The experiments were performed at room temperature in liquid
191 conditions, particularly in ethanol. AFM nanoindentation requires precise knowledge of the
192 cantilever sensitivity. In order to evaluate this parameter, the calibration procedure consists in
193 pressing the AFM tip onto an 'infinitely hard' surface, and to measure the gradient of the
194 vertical displacement of cantilever versus the photodiode signal caused by the cantilever
195 deflection (Clifford & Seah, 2005). Finally, once the system is perfectly calibrated, AFM
196 nanoindentation can be performed on particle powders. A camera allows to visualize the
197 sample and to select a particle powder. Once above the selected particle, the tip is put in
198 contact with the surface and the measurements are initiated.

199 (2) Mechanical properties of particle powder surface was obtained by recording force-
200 indentation curves. To perform nanoindentation tests, the AFM is operated in force mode and
201 the tip is brought into contact with the surface, pushed to a maximum load (Approach curve),
202 and then withdrawn (withdrawal curve). The voltage on the photodiode is recorded during the
203 movement and plotted against the vertical distance to the sample. The voltages recorded can
204 be converted into forces by Hooke's law thus providing force-distance curves. Force/volume
205 images consisting of 16×16 force curves were recorded for a $20 \mu\text{m} \times 20 \mu\text{m}$ scanned
206 surface meaning that a pixel has a dimension of $1.25 \mu\text{m} \times 1.25 \mu\text{m}$.

207 (3) During nanoindentation measurements, force curves are recorded and converted into
208 force versus indentation curves using appropriate treatments (Burnham & Colton, 1989).
209 Force curves were exported as ASCII files and processed with a custom program written in
210 Matlab (MathWorks, Inc., Natick, MA). The measured force-indentation curves were
211 processed to estimate the Young's modulus (also known as the elastic modulus) of the
212 sample. The Young's modulus was obtained by applying Hertz theory for elastic media
213 (Hertz, 1882) and elasticity maps were designed.

$$(4) F = \frac{2E \tan\alpha}{\pi(1-\nu^2)} \delta^2 \quad (2)$$

214 where F is the force, δ the indentation depth, E the Young modulus, ν the Poisson coefficient
215 and α the semi-top angle of the tip.

216 Finally, analysis of at least three elasticity maps provided a mean elasticity value for each
217 analyzed sample.

218

219 **3. Results and discussion**

220 **3.1. Surface composition and structure of MC powders**

221 Dairy powders surface is essential in its functional properties (Crowley, Kelly, Schuck,
222 Jeantet & O'mahony, 2016), such as rehydration ability, which is crucial for the end use of a
223 product. Surface composition of MC powders was determined by XPS on fresh and aged
224 samples. XPS results are presented in **Figure S1**. Overall, no significant differences in surface
225 composition were evidenced between analyzed samples. However, because XPS provides
226 composition on large surface area, very local modifications cannot be revealed by this
227 technique. Images of particle structure and surface topography were acquired by SEM. As
228 displayed in **Figure 2**, particle sizes were heterogeneous and their surface appeared smooth in
229 spite of the presence of dents. Regarding surface topography of fresh and aged powders, no
230 differences were noticed, confirming previous observations reported in the literature (Fäldt &
231 Bergenståhl, 1996; Fyfe et al., 2011). Unexpectedly, AFM topographical measurements
232 revealed an increase in surface roughness during powder aging (**Figure 3**). These little
233 variations were not discernible on SEM observation maybe because of the iridium coating that
234 is thicker than 5 nm, which may have overlay differences in surface profiles of fresh and aged
235 powders. On the contrary, AFM in contact mode is highly sensitive to very fine topographical
236 deviations. R_a was calculated according to equation 1, and gave values of 5.1 ± 0.8 nm for the
237 fresh powder and 7.8 ± 0.8 nm for the MC powder stored for 10 months at 40 °C. Statistical

238 analysis evidenced that roughness was significantly different ($p \leq 0.01$). In particular, as can
239 be noticed on the 3D representation (**Figure 3**), many hollows of around 500 nm diameter
240 were noticeable on particle surface after aging at 40 °C for 10 months, while slight variations
241 in roughness were observed on fresh particle powder surface.

242

243 **3.2. Nanomechanical properties of MC powder surface**

244 Nanomechanical properties of MC powder surface were explored using AFM nanoindentation
245 measurements. Force/indentation curves were analyzed using the Hertz theory to generate
246 elasticity maps (**Figure 4 - inserts**). The colorbar associates low elasticity values when the
247 region is purple and high elasticity values when the region is red. The average of elasticity
248 values obtained in three maps was used to calculate the mean elasticity of fresh and aged
249 powders (**Figure 4**). The fresh powder presented a mean elasticity of 0.16 ± 0.03 GPa which
250 is lower than values obtained for NPC skin layers (0.48 ± 1.10^{-3} GPa) by applying indentation
251 test (Sadek et al., 2015) but from the same order. These differences can be explained by the
252 system studied itself, a protein layer for Sadek et al., (2015) versus a particle powder in the
253 present study. Also drying conditions were not identical between the two systems. In
254 nanoindentation test, the length scale of the penetration is smaller than for an indentation test
255 meaning that thanks to AFM nanoindentation the extreme surface was probed. The initial
256 elasticity map revealed that surface is homogeneous as already supposed by Sadek et al.,
257 (2015) for skin layers. It was impossible to find the technique applied to systems similar as
258 ours. But, AFM nanoindentation was performed on pharmaceutical powders and for example
259 lactose powders exhibited values that were comprised between 0.18 and 0.51 GPa (Masterson
260 & Cao, 2008) which is not far from the elasticity values obtained on MC powders in the
261 present work. Elasticity maps recorded on stored powders were totally different: not
262 homogeneous with local harder surfaces. Nonetheless, it is important to remember that the

263 size of a pixel in these maps is $1.25 \mu\text{m} \times 1.25 \mu\text{m}$ meaning that unfortunately differences in
264 elasticity cannot be attributed to topographical modification. For future work, it could be
265 interesting to improve resolution in order to highlight very local modifications on powder
266 surface. Elasticity increase during storage is a consequence of particle surface hardening:
267 indeed, fresh MC powder had a relatively soft surface at the beginning of the storage, which
268 evolved into a stiffer surface with elasticity values of 18.85 ± 9.33 after 10 months storage at
269 $40 \text{ }^\circ\text{C}$.

270

271 **3.3. Evolution of surface structure during powder rehydration**

272 The three-dimensional organization of the material on particle surface was considerably
273 modified during rehydration (**Figure 5**).

274 *Short term rehydration.*

275 Under short term rehydration, fresh MC powders globally followed the behavior described by
276 Mimouni et al. (Mimouni, Deeth, Whittaker, Gidley & Bhandari, 2010a). Their microstructure
277 was characterized by a loose assembly of individual casein micelles. For aged MC powders
278 that were stored during 6 months at $40 \text{ }^\circ\text{C}$, particles appeared poorly affected by the
279 rehydration media and casein micelles were tighter on particle surface. On fresh and 6-month
280 aged MC powders, the remaining undissolved powder particles presented large holes of
281 several micrometers within the surface. These holes resulted from partial material removal
282 upon rehydration, leading to the release of surface casein micelles in the surrounding media.
283 Slow rehydration of dairy powders is often attributed to the casein fraction, known to have a
284 poor dispersibility, and this phenomenon may be enhanced after storage at elevated
285 temperature (Mimouni, Deeth, Whittaker, Gidley & Bhandari, 2010a). Finally, for prolonged
286 storage of MC powders (10 months at $40 \text{ }^\circ\text{C}$), the particle surface appeared almost unaffected
287 by the rehydration media (no individual casein micelles can be observed) and looked like a

288 dry powder. Likewise, the large holes described for fresh and 6-month stored MC powders are
289 no longer noticeable on particles stored for ten months at 40 °C.

290 *Long term rehydration.*

291 The long term rehydration process was conducted during 1 hour and particle surface was
292 again analyzed. Only residual material was observed after long term rehydration of the fresh
293 powder, while particles remained visible for powders stored at 40 °C. However, surface
294 hydration after long term rehydration seemed to decrease with storage duration. In particular,
295 as for short term rehydration, particles of the 10-month aged powder seem almost unaffected
296 by the rehydration media. In the intermediate case (6-month aged powder), particles were far
297 from fully solubilized but their surface appeared significantly hydrated with the presence of
298 individual casein micelles. Approaching more finely the particle surface was possible by the
299 exceptional resolution properties of a high-resolution field-emission SEM. The rehydration of
300 a fresh MC powder allows visualizing casein micelles arranged in an open gel-like
301 organization (Mimouni, Deeth, Whittaker, Gidley & Bhandari, 2010a). On the contrary, the
302 aged powder stored for 6 months at 40 °C presented a layer of tightly packed casein micelles.
303 Finally, when the powder was stored for 10 months at 40 °C, the integrity of particle surface
304 seemed preserved (no holes could be observed) and the previously described casein micelles
305 assemblies were not noticeable. Only the fresh MC powder succeeded to rehydrate, whereas
306 rehydration capacity of aged powders was markedly affected by storage.

307 Dynamic vapor sorption (DVS) is an interesting tool to evaluate the ability of powders to
308 adsorb water (Schuck, Dolivet & Jeantet, 2012). The method provide information on the
309 rehydration of a dry product through adsorption isotherm. Gaiani et al. (2006) investigated the
310 effect of storage on surface composition, water sorption properties and powder microstructure
311 of MC powders. A significant decreased of the monolayer water capacity was noticed by
312 these authors on the same powders during storage for 60 days at 50 °C (around 0.0632 kg.kg⁻¹

313 for fresh and around $0.0524 \text{ kg.kg}^{-1}$ for aged MC powders). MC powders are the milk
314 powders able to absorb the highest quantities of water in a fresh state. In the present study,
315 water sorption properties were also evaluated (data not shown) and same tendencies were
316 obtained (around $0.0644 \text{ kg.kg}^{-1}$ for fresh and around $0.0424 \text{ kg.kg}^{-1}$ for aged MC powders).
317 This implies that the ability of aged powder to adsorb water is affected compared to fresh
318 powders which is in accordance with the SEM observation (**Figure 5**). This impossibility to
319 absorb elevated quantities of water can be related to the structural modifications of the
320 micelles observed.

321 From SEM analysis, it can be stated that the powder particle surface is not uniformly affected
322 by the rehydration media, but some parts are solubilised while other parts remain unaffected.
323 This spatial heterogeneity of particle rehydration meaning that partial removal of the crust
324 occurred during rehydration has previously been described (Mimouni, Deeth, Whittaker,
325 Gidley & Bhandari, 2010a). Additionally, heterogeneity in rehydration behavior was also
326 denoted for the first time between particles from a same batch. More precisely, the hydration
327 degree of particle surface was totally different, ranging from well to poorly hydrated (**Figure**
328 **6**). These differences between individual particles could be the result of different residence
329 time of the product in the dryer. It was shown that for a three-stage installation, depending on
330 configurations related to fine particle recycling, some powder particles could leave the tower
331 almost immediately, whilst others could remain in the installation for more than 70 min
332 (Jeantet, Ducept, Dolivet, Méjean & Schuck, 2008).

333

334 **3.4 Proposed mechanism of modification during powder storage**

335 Complete rehydration is a crucial step for the effective expression of protein functionality
336 (Crowley et al., 2015). The inhibition of water transfer inside particles is the limiting factor
337 during rehydration of powders of high protein content, especially when caseins are the

338 predominant proteins. The long time required for complete rehydration was attributed to the
339 slow dispersion of a “skin” of casein micelles present at particle surfaces (Mimouni, Deeth,
340 Whittaker, Gidley & Bhandari, 2009). Numerous authors consider that the slow dispersion of
341 primary particles is responsible for the extended rehydration times of casein-dominant
342 powders (Fang, Selomulya, Ainsworth, Palmer & Chen, 2011; Gaiani, Banon, Scher, Schuck
343 & Hardy, 2005; Richard, et al., 2013). In their work, Scokker *et al.* (2011) improved the
344 powder reconstitutability by increasing the amount of non-micellar protein in the spray-drying
345 feed. Two possible mechanisms contributing to the positive effect of non-micellar casein were
346 highlighted. One of them proposes the spatial separation of the casein micelles by non-
347 micellar casein, preventing micelle–micelle interactions which can contribute to reduce the
348 incidence of micelle cross-linking. The present study suggests that the apparent surface
349 structure of powder particles during rehydration results from modification occurring during
350 storage. Up to now, exact mechanisms behind these observations were never evidenced but
351 AFM in topographical and force mode used in the present work can help in the development
352 of some assumptions (**Figure 7**). In fresh powders, casein micelles are spatially separated thus
353 preventing cross-linking between caseins. After storage at high temperature, aggregation of
354 casein micelles leads to heterogeneous surface where caseins are tighter and this phenomenon
355 may generate the mentioned hollows that were observed on topographical measurements.
356 From a mechanical point of view, this results in an increase of elastic modulus reflecting a
357 harder surface for aged powders. Hardening is a time-dependent, restructuring process
358 occurring in concentrated systems (Hogan, O'Loughlin & Kelly, 2016). The proposed
359 mechanisms underlying are protein aggregation through covalent (intermolecular disulphide
360 bonds) and non-covalent (hydrophobic) interactions that can results in harder surface (Zhou,
361 Liu & Labusa, 2008). Moreover, surface hardening during storage at elevated temperature
362 resembles to shrinkage and case-hardening phenomenon occurring during drying of food

363 materials (Gulati & Datta, 2015). Drying of food materials usually results in large
364 deformations (shrinkage) due to moisture removal. Material shrinkage (or strains) results in
365 stress development that plays a critical role in the development of food structure and final
366 volume of the dried product.

367

368 **4. Conclusion**

369 The measurement of nanomechanical properties of MC particle surface by AFM
370 nanoindentation revealed an increase in surface hardness during storage at high temperature,
371 while particle surface topography was barely affected. However, particle behavior during
372 rehydration was markedly affected by storage conditions, leading to a compact network of
373 casein micelles for aged powders, while it was looser for fresh powders. Nanomechanics
374 revealed particle surface modifications during storage that were not visible on SEM images
375 but having a great influence on powder ability to rehydrate. The harder particle surface
376 observed for aged powders can be the result of compacted micelles, a material that is further
377 difficult to disperse, resulting in very low rehydration mechanisms. The main reason for this
378 reduction of powder solubility could be the non-covalent aggregation of closely-packed casein
379 micelles. Finally, the hollow structures observed on topographical images (AFM) at dry state
380 may originate from protein aggregation and resulting to a harder surface demonstrated by
381 nanomechanical measurements. These modification can explain why powder rehydration is
382 tricky after storage.

383

384 **5. Acknowledgements**

385 The authors thank the French Dairy Interbranch Organization (CNIEL). The authors
386 acknowledge the facilities, as well as the scientific and technical assistance provided by the
387 School of Agriculture and Food Sciences (SAFS) at The University of Queensland and the

388 Australian Microscopy & Microanalysis Research Facility at the Centre for Microscopy and
389 Microanalysis (CMM, The University of Queensland).

390

391 6. References

392 Anema, S., Pinder, D., Hunter, R., & Hemar, Y. (2006). Effects of storage temperature on the
393 solubility of milk protein concentrate (MPC85). *Food Hydrocolloids*, 20(2), 386-393.

394 Baldwin, A. J. (2010). Insolubility of milk powder products—A minireview. *Dairy Science &*
395 *Technology*, 90(2-3), 169-179.

396 Burnham, N. A., & Colton, R. J. (1989). Measuring the nanomechanical properties and
397 surface forces of materials using an atomic force microscope. *Journal of Vacuum*
398 *Science & Technology A*, 7(4), 2906-2913.

399 Cao, X., Morganti, M., Hancock, B. C., & Masterson, V. M. (2010). Correlating particle
400 hardness with powder compaction performance. *Journal of pharmaceutical sciences*,
401 99(10), 4307-4316.

402 Clifford, C. A., & Seah, M. P. (2005). Quantification issues in the identification of nanoscale
403 regions of homopolymers using modulus measurement via AFM nanoindentation.
404 *Applied surface science*, 252(5), 1915-1933.

405 Crowley, S., Kelly, A., Schuck, P., Jeantet, R., & O'mahony, J. (2016). Rehydration and
406 solubility characteristics of high-protein dairy powders. In *Advanced Dairy*
407 *Chemistry* (pp. 99-131): Springer.

408 Crowley, S. V., Desautel, B., Gazi, I., Kelly, A. L., Huppertz, T., & O'Mahony, J. A. (2015).
409 Rehydration characteristics of milk protein concentrate powders. *Journal of Food*
410 *Engineering*, 149, 105-113.

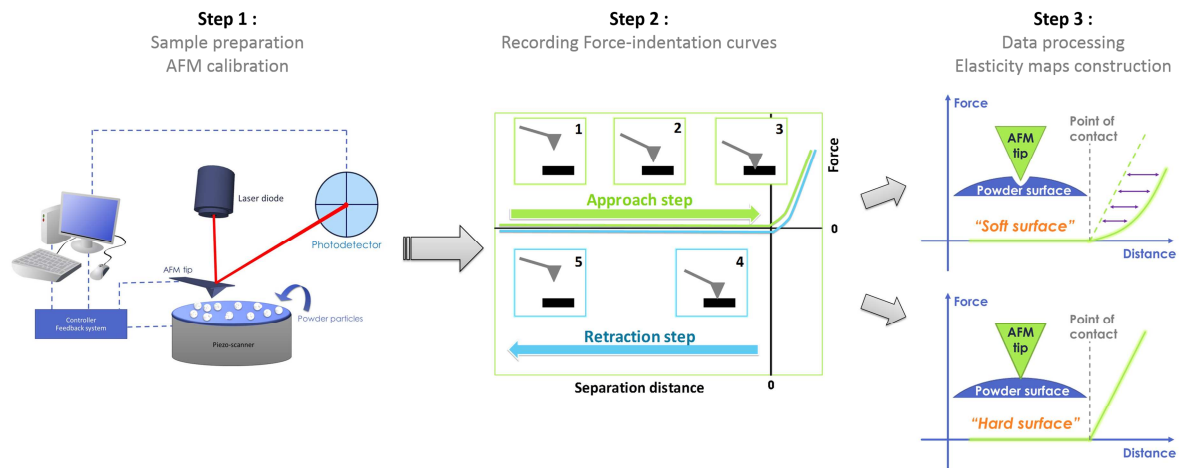
- 411 Dalgleish, D. G., Spagnuolo, P. A., & Goff, H. D. (2004). A possible structure of the casein
412 micelle based on high-resolution field-emission scanning electron microscopy.
413 *International Dairy Journal*, 14(12), 1025-1031.
- 414 Fäldt, P., & Bergenståhl, B. (1996). Spray-dried whey protein/lactose/soybean oil emulsions.
415 1. Surface composition and particle structure. *Food Hydrocolloids*, 10(4), 421-429.
- 416 Fang, Y., Selomulya, C., Ainsworth, S., Palmer, M., & Chen, X. D. (2011). On quantifying
417 the dissolution behaviour of milk protein concentrate. *Food Hydrocolloids*, 25(3),
418 503-510.
- 419 Fang, Y., Rogers, S., Selomulya, C., & Chen, X. D. (2012). Functionality of milk protein
420 concentrate: Effect of spray drying temperature. *Biochemical Engineering Journal*,
421 62, 101-105.
- 422 Fischer-Cripps, A. C. (2000). Introduction to contact mechanics. New York: Springer.
- 423 Fyfe, K. N., Kravchuk, O., Le, T., Deeth, H. C., Nguyen, A. V., & Bhandari, B. (2011).
424 Storage induced changes to high protein powders: influence on surface properties
425 and solubility. *Journal of the Science of Food and Agriculture*, 91(14), 2566-2575.
- 426 Gaiani, C., Banon, S., Scher, J., Schuck, P., & Hardy, J. (2005). Use of a turbidity sensor to
427 characterize micellar casein powder rehydration: Influence of some technological
428 effects. *Journal of Dairy Science*, 88(8), 2700-2706.
- 429 Gaiani, C., Ehrhardt, J., Scher, J., Hardy, J., Desobry, S., & Banon, S. (2006). Surface
430 composition of dairy powders observed by X-ray photoelectron spectroscopy and
431 effects on their rehydration properties. *Colloids and Surfaces B: Biointerfaces*, 49(1),
432 71-78.
- 433 Gaiani, C., Scher, J., Ehrhardt, J. J., Linder, M., Schuck, P., Desobry, S., & Banon, S. (2007).
434 Relationships between dairy powder surface composition and wetting properties

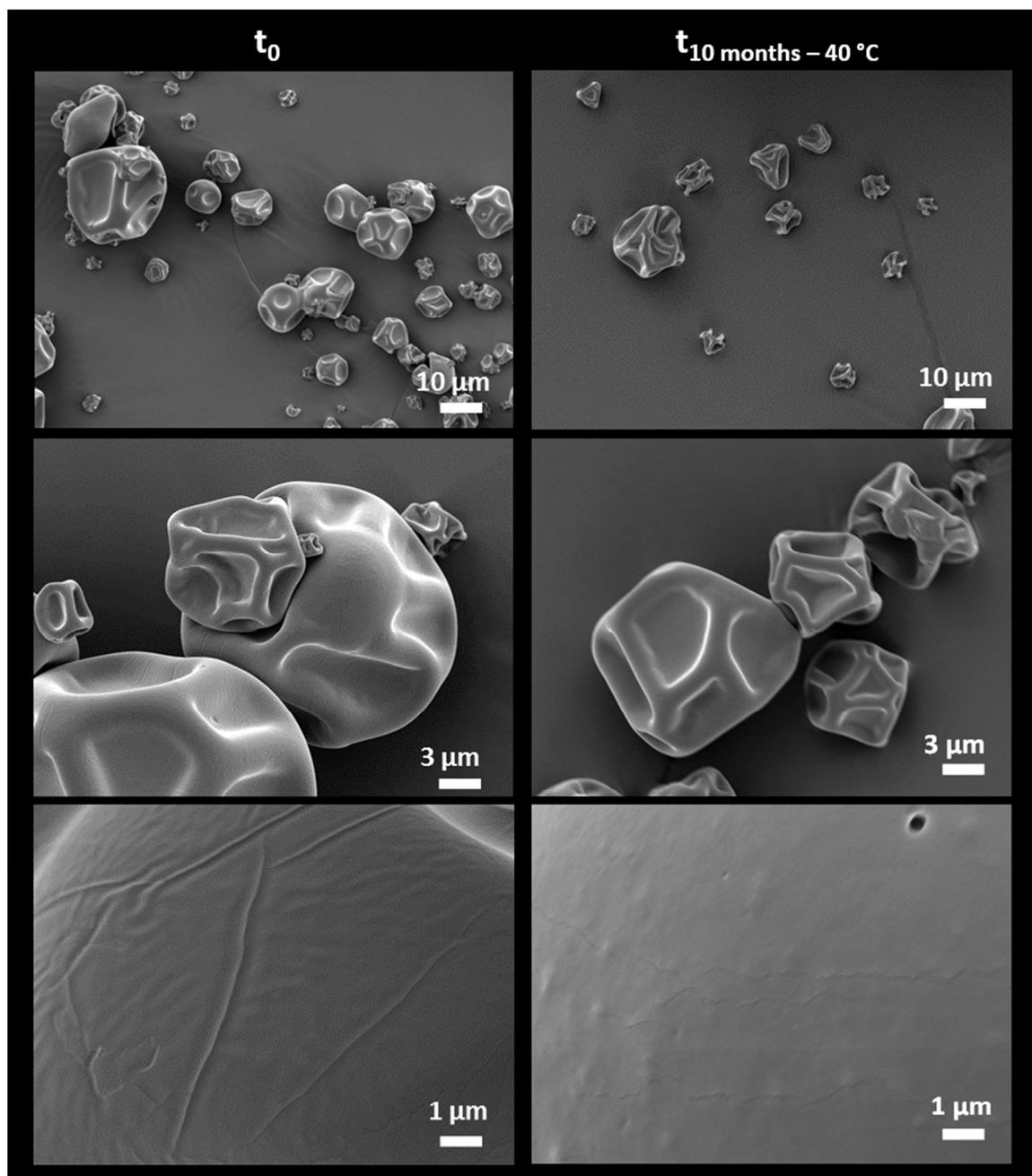
- 435 during storage: importance of residual lipids. *Journal of agricultural and food*
436 *chemistry*, 55(16), 6561-6567.
- 437 Gaiani, C., Schuck, P., Scher, J., Desobry, S., & Banon, S. (2007). Dairy Powder
438 Rehydration: Influence of Protein State, Incorporation Mode, and Agglomeration.
439 *Journal of Dairy Science*, 90(2), 570-581.
- 440 Gazi, I., & Huppertz, T. (2015). Influence of protein content and storage conditions on the
441 solubility of caseins and whey proteins in milk protein concentrates. *International*
442 *Dairy Journal*, 46, 22-30.
- 443 Gulati, T., & Datta, A. K. (2015). Mechanistic understanding of case-hardening and texture
444 development during drying of food materials. *Journal of Food Engineering*, 166,
445 119-138.
- 446 Haque, E., Whittaker, A. K., Gidley, M. J., Deeth, H. C., Fibrianto, K., & Bhandari, B. R.
447 (2012). Kinetics of enthalpy relaxation of milk protein concentrate powder upon
448 ageing and its effect on solubility. *Food chemistry*, 134(3), 1368-1373.
- 449 Havea, P. (2006). Protein interactions in milk protein concentrate powders. *International*
450 *Dairy Journal*, 16(5), 415-422.
- 451 Hertz, H. (1882). Über die Berührung fester elastischer Körper.
- 452 Hogan, S. A., O'Loughlin, I. B., & Kelly, P. M. (2016). Soft matter characterisation of whey
453 protein powder systems. *International Dairy Journal*, 52, 1-9.
- 454 Jeantet R., Ducept F., Dolivet A., Méjean S. & Schuck P. (2008). Residence time
455 distribution : a tool to improve spray-drying control. *Dairy Science & Technology*,
456 88(1), 31-43.
- 457 Kasas, S., Longo, G., & Dietler, G. (2013). Mechanical properties of biological specimens
458 explored by atomic force microscopy. *Journal of Physics D: Applied Physics*,
459 46(13), 133001.

- 460 Kelly, A. L., & Fox, P. F. (2016). Manufacture and Properties of Dairy Powders. In
461 *Advanced Dairy Chemistry* (pp. 1-33): Springer.
- 462 Le, T. T., Bhandari, B., & Deeth, H. C. (2011). Chemical and physical changes in milk
463 protein concentrate (MPC80) powder during storage. *Journal of agricultural and*
464 *food chemistry*, 59(10), 5465-5473.
- 465 Le, T. T., Bhandari, B., Holland, J. W., & Deeth, H. C. (2011). Maillard reaction and protein
466 cross-linking in relation to the solubility of milk powders. *Journal of agricultural*
467 *and food chemistry*, 59(23), 12473-12479.
- 468 Levy, R., & Maaloum, M. (2002). Measuring the spring constant of atomic force microscope
469 cantilevers: thermal fluctuations and other methods. *Nanotechnology*, 13(1), 33.
- 470 Liao, X., & Wiedmann, T. S. (2004). Characterization of pharmaceutical solids by scanning
471 probe microscopy. *Journal of pharmaceutical sciences*, 93(9), 2250-2258.
- 472 Masterson, V. M., & Cao, X. (2008). Evaluating particle hardness of pharmaceutical solids
473 using AFM nanoindentation. *International Journal of Pharmaceutics*, 362(1-2), 163-
474 171.
- 475 Mimouni, A., Deeth, H. C., Whittaker, A. K., Gidley, M. J., & Bhandari, B. R. (2009).
476 Rehydration process of milk protein concentrate powder monitored by static light
477 scattering. *Food Hydrocolloids*, 23(7), 1958-1965.
- 478 Mimouni, A., Deeth, H., Whittaker, A., Gidley, M., & Bhandari, B. (2010a). Investigation of
479 the microstructure of milk protein concentrate powders during rehydration:
480 alterations during storage. *Journal of Dairy Science*, 93(2), 463-472.
- 481 Mimouni, A., Deeth, H. C., Whittaker, A. K., Gidley, M. J., & Bhandari, B. R. (2010b).
482 Rehydration of high-protein-containing dairy powder: Slow-and fast-dissolving
483 components and storage effects. *Dairy Science & Technology*, 90(2-3), 335-344.

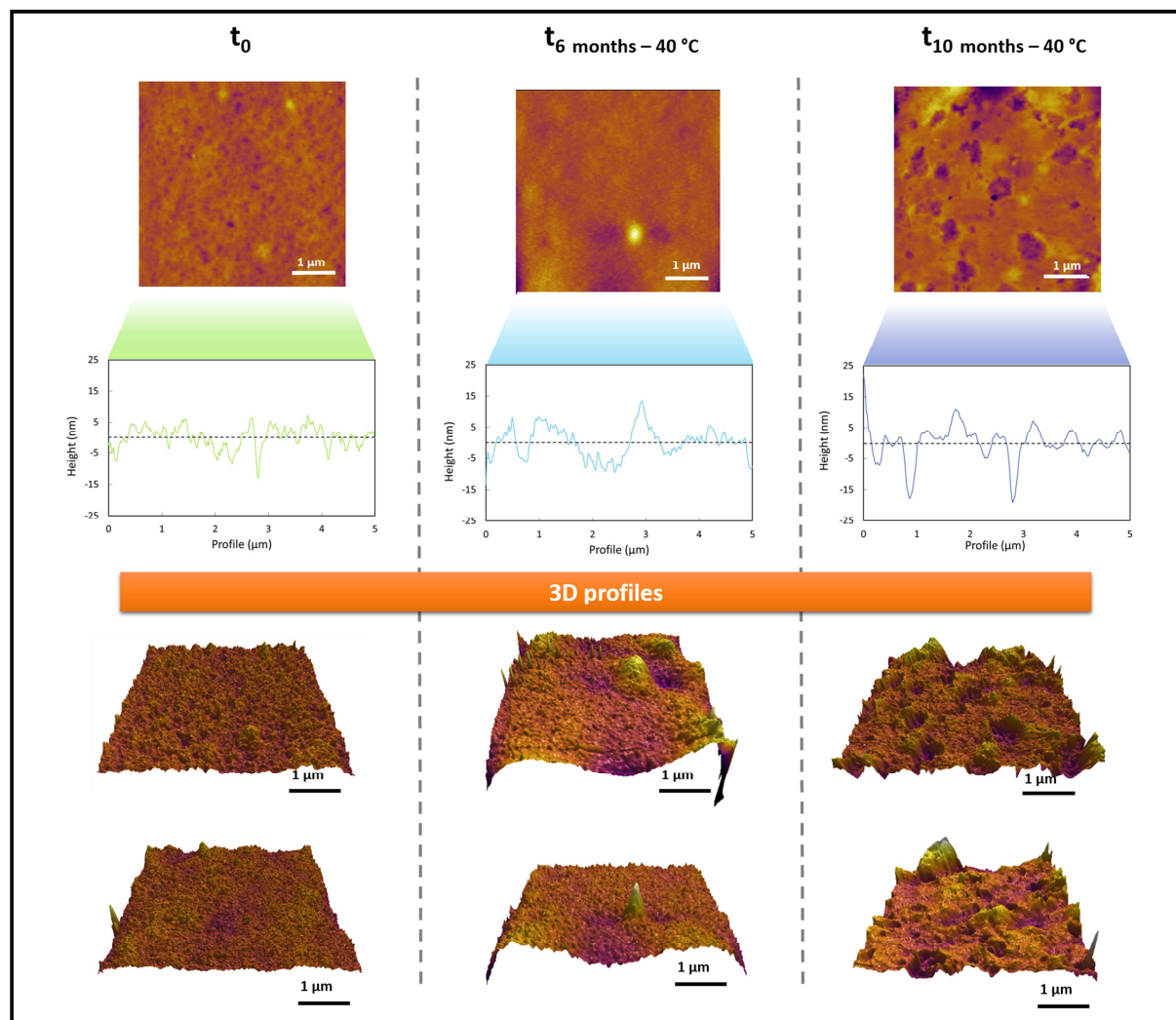
- 484 Perkins, M., Ebbens, S. J., Hayes, S., Roberts, C. J., Madden, C. E., Luk, S. Y., & Patel, N.
485 (2007). Elastic modulus measurements from individual lactose particles using atomic
486 force microscopy. *International Journal of Pharmaceutics*, 332(1), 168-175.
- 487 Pierre, A., Fauquant, J., Le Graet, Y., Piot, M., & Maubois, J. (1992). Préparation de
488 phosphocaséinate natif par microfiltration sur membrane. *Le Lait*, 72(5), 461-474.
- 489 Ramos, K., & Bahr, D. (2007). Mechanical behavior assessment of sucrose using
490 nanoindentation. *Journal of materials research*, 22(07), 2037-2045.
- 491 Richard, B., Le Page, J.-F., Schuck, P., Andre, C., Jeantet, R., & Delaplace, G. (2013).
492 Towards a better control of dairy powder rehydration processes. *International Dairy*
493 *Journal*, 31(1), 18-28.
- 494 Rollema, H. S. & Muir, D. D. (2009). 6 Casein and Related Products. Dairy powders and
495 concentrated products, 235.
- 496 Rouxhet, P. G., Misselyn-Bauduin, A. M., Ahimou, F., Genet, M. J., Adriaensen, Y., Desille,
497 T., Bodson, P. & Deroanne, C. (2008). XPS analysis of food products: toward
498 chemical functions and molecular compounds. *Surface and Interface Analysis*, 40(3-
499 4), 718-724.
- 500 Sadek, C., Pauchard, L., Schuck, P., Fallourd, Y., Pradeau, N., Le Floch-Fouéré, C., &
501 Jeantet, R. (2015). Mechanical properties of milk protein skin layers after drying:
502 Understanding the mechanisms of particle formation from whey protein isolate and
503 native phosphocaseinate. *Food Hydrocolloids*, 48, 8-16.
- 504 Schokker, E. P., Church, J. S., Mata, J. P., Gilbert, E. P., Puvanenthiran, A., & Udabage, P.
505 (2011). Reconstitution properties of micellar casein powder: Effects of composition
506 and storage. *International Dairy Journal*, 21(11), 877-886.

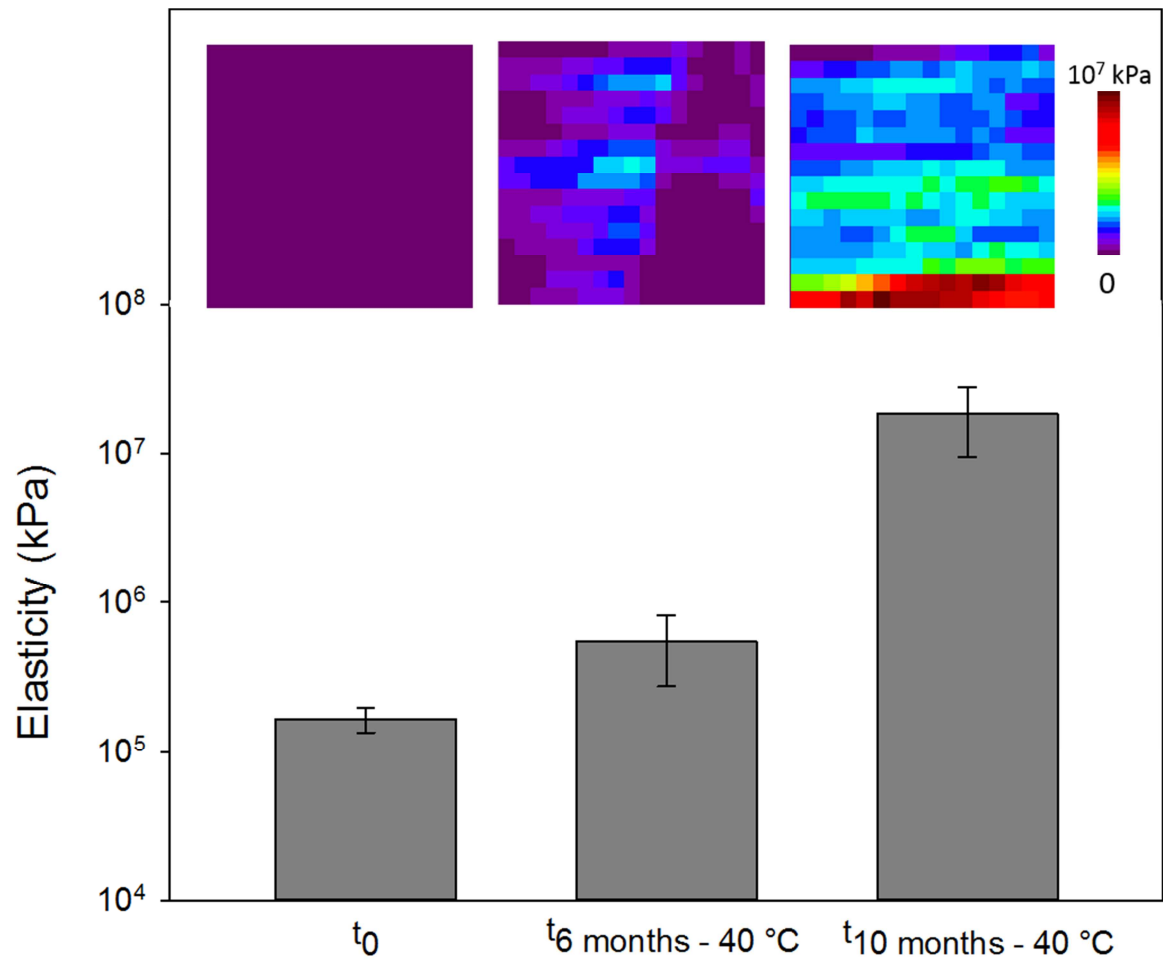
- 507 Schuck, P., Piot, M., Méjean, S., Le Graet, Y., Fauquant, J., Brulé, G., & Maubois, J. (1994).
508 Déshydratation par atomisation de phosphocéinate natif obtenu par microfiltration
509 sur membrane. *Le Lait*, 74(5), 375-388.
- 510 Schuck, P., Dolivet, A., & Jeantet, R. (2012). Analytical methods for food and dairy
511 powders. Wiley-Blackwell, Oxford
- 512 Wu, X., Li, X., & Mansour, H. M. (2010). Surface analytical techniques in solid-state particle
513 characterization for predicting performance in dry powder inhalers. *KONA Powder
514 and Particle Journal*, 28(0), 3-19.
- 515 Zhou, P., Liu, X., & Labuza, T. P. (2008). Effects of moisture-induced whey protein
516 aggregation on protein conformation, the state of water molecules, and the
517 microstructure and texture of high-protein-containing matrix. *Journal of agricultural
518 and food chemistry*, 56(12), 4534-4540.



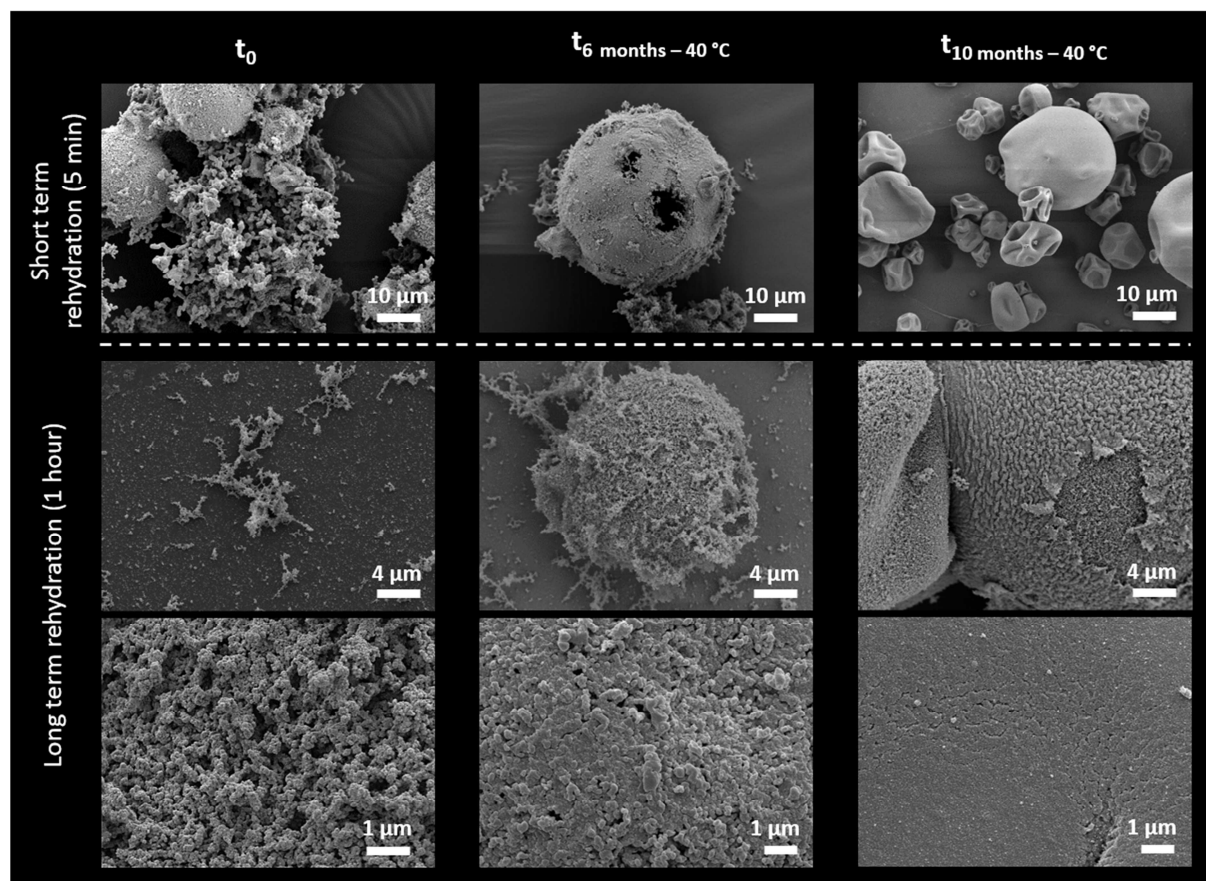


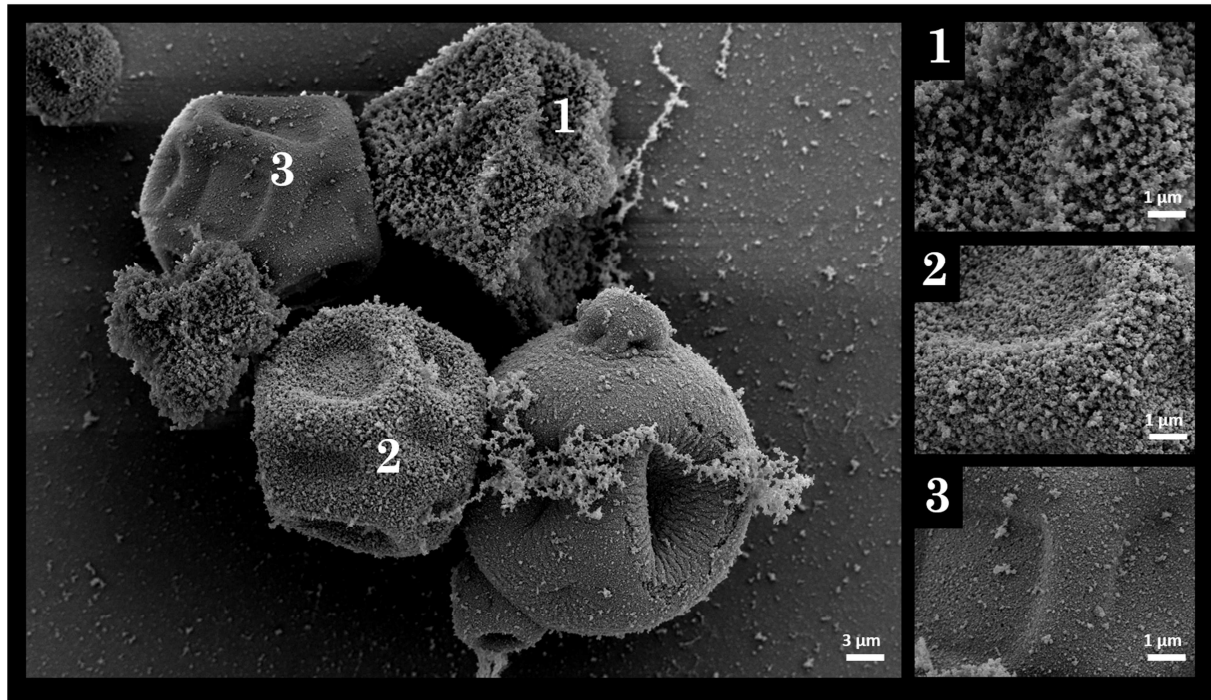
ACC



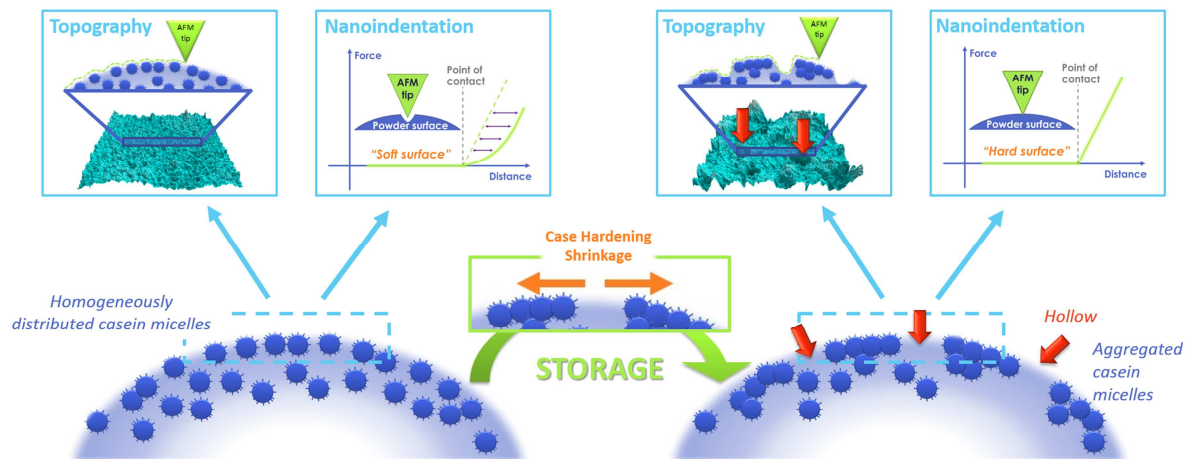


ACCEPTED





ACCEPTED MANUSCRIPT



- MC powder presents hollow zones and harder surface during storage
- Storage induce loss of rehydration ability of MC powder
- Surface hydration is heterogeneous between particles from a same powder batch

ACCEPTED MANUSCRIPT